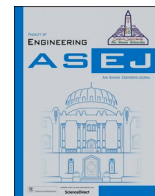




Contents lists available at ScienceDirect

Ain Shams Engineering Journal

journal homepage: www.sciencedirect.com

Full Length Article

Performance enhancing of porcelain insulators using low cost micro additives

Hesham S. Karaman^{a,*}, Sherif M.M. Sherif^a, S.M.A. El-Gamal^b, Naser Abdel-Rahim^c, M.A. Abd-Allah^a

^a Faculty of Engineering at Shoubra, Benha University, Egypt

^b Faculty of Science, Ain Shams University, Egypt

^c Future University, Egypt

ARTICLE INFO

Keywords:

Dielectric properties
Porcelain insulators
Breakdown strength
Dissipation factor
Porosity

ABSTRACT

Porcelain have been widely utilized in electrical power system. The enhancement of its properties has positively influenced its behavior thence on overall power system. Nano/Micro technologies are influential field used for developing different characteristics of porcelain insulators. In this work, three weight percentages of fly ash micro-particles were admixed to neat porcelain. Characterization and morphological features for prepared samples were scrutinized using XRD and SEM. BDV, relative permittivity, and dissipation factor were measured. Moreover, porosity, bulk density, and water absorption were measured. COMSOL Software was used to simulate the electric field distribution on the samples. This study indicated, fly ash promoted the electrical characteristics of porcelain. Inclusion of 6 % fly ash along the porcelain sample increases BDV from 22.5 kV to 56.7 kV. The presence of fly ash inside porcelain not only decreased relative permittivity but also dissipation factor. The optimum sintering temperature gives lowest porosity and highest bulk density was 1200 °C.

1. Introduction

The development of the electrical insulators (gases, liquids, and solids) is highly important issue that directly impact on the overall state of the electrical power system. these improvement and development processes provide many enhancing approaches for the power system as; best performance, long life time, continuity of supply, damage minimization, and lower maintenance requirements. Accordingly, many researchers interested to study the different operations that enhance the dielectrics characteristics. one of these, the addition of nano or micro materials into the base insulating material. there are many processes to prepare this insulating material based on these nano or micro additives. these processes may be physical or chemical process or both. each researcher makes characterization processes using XRD, SEM, TEM, and so on to evaluate the quality of the sample preparation. then, researcher tests the prepared samples to investigate and discuss the results that obtained.

Regarding to solid dielectrics, porcelain insulators have been widely utilized in the electrical power grid. The most popular applications for porcelain insulators in the transmission and distribution systems appear

as overhead transmission lines carriers and in power transformers bushings. The major function of these insulators (porcelain) is to insulate the high voltage conductors from support structures [1,2]. The insulation failure is one of the most reasons that threaten the continuity of the electrical supply and power grid reliability. Thence, the amelioration of the dielectric and physical properties of porcelain insulators is necessary for positive reflection on power grid performance [3]. Recently, many studies have been investigated to develop the performance of porcelain materials as the most popular solid insulators [4-6]. The aim of these studies is the improving of the different characteristics of the porcelain insulators using nano/micro compositions [7-10]. Related to the dielectric properties of the porcelain insulator, Belhouche et al. concluded that the addition of waste glass with certain quantities provides an enhancement in the dielectric properties of porcelain insulators [3]. Desouky et al. added nano-silica to porcelain material and achieved improvement for the breakdown voltage and relative permittivity [11]. TiO₂ nanoparticles used to ameliorate the characteristics of porcelain insulators investigated by Zhuang et al., the results revealed that coating of TiO₂ films on the porcelain insulator surface enhances the AC flashover voltage with 6 % compared to an uncoated insulator [12].

* Corresponding author.

E-mail addresses: hesham.said@feng.bu.edu.eg (H.S. Karaman), naser.abdelrahim@fue.edu.eg (N. Abdel-Rahim).

<https://doi.org/10.1016/j.asej.2023.102622>

Received 16 September 2023; Received in revised form 25 November 2023; Accepted 22 December 2023

2090-4479/© 2023 THE AUTHORS. Published by Elsevier BV on behalf of Faculty of Engineering, Ain Shams University. This is an open access article under the CC BY-NC-ND license (<http://creativecommons.org/licenses/by-nc-nd/4.0/>).

On the other hand, related to the physical properties of porcelain insulators, the insertion of glass particles into the porcelain matrix reduces the porosity and the water absorption with the increment of the mass percentage of the glass additives [3]. Desouky et al. presented that, the equipping of nano-silica into the blank porcelain enhances the physical characteristics and the thermal properties of the porcelain material [11]. Wu et al. studied the effect of boron nitride (BN) nano-additives (10 & 40 wt%) on the thermal properties of outdoor insulators. The reported results pointed that the insulator thermal conductivity was increased by about 75 % due to the addition of BN also; the weather resistance and the heat corrosion were improved [13].

Several researchers were employed to develop and ameliorate the dielectric and physical properties of porcelain insulators using different nanomaterials and it is well known that nanomaterials have valuable cost. So, this work aspires to develop porcelain insulators using low cost additives. The preparation of porcelain samples in this work were done using economic raw materials (kaolin, feldspar, and quartz). Fly ash micro scale material (solid waste material) was added to neat porcelain to prepare the different developed porcelain composites. Fly ash is considered as the main industrial powdery waste (solid wastes) produced from the burning process of solid fuels. The main constituted of fly ash are unburned carbon, SiO_2 , Fe_2O_3 , CaO , and Al_2O_3 , and other minor inorganic substances [14]. Fly ash microparticles were added by different weight percentage to porcelain material. Breakdown voltage, relative permittivity, dissipation factor, porosity, bulk density, and water absorption were measured for the prepared samples to excogitate the porcelain material dielectric and physical properties. Moreover, COMSOL Multiphysics Software was used to simulate the distribution of electric field on the porcelain samples at the values of the measured breakdown voltage.

2. Samples preparation

In this work, different porcelain composites were experimental prepared using 0, 2, 4, and 6 wt% of fly ash micro-particles. The blank porcelain sample (BPS) was first prepared by the wet mixing of kaolin, feldspar, and quartz with weight ratios 2:1:1; respectively and ball milling for 3 h in porcelain ball mill. The used weight ratios are according to the previously published research [11]. The sample had been sieved using magnetic sieve (200 μm) to remove the minor quantities of impurities that still present. Finally, the sample was dried for a day at 110 °C, ground finely and sieved through a sieve of 200 μm . For specimens' preparation 100 g of this sample was mixed with ~ 10 ml water and 10 g were stamped by compressive strength machine at 50–60 MPa. The obtained specimens (in shape of discs with 2 cm diameter and 2 mm thickness) were dried at 100 °C in an oven for 1 day. After this drying process, the sample was burned for 2 h at 1100 °C, 1200 °C, 1300 °C and 1400 °C, and left to cool to ambient temperature before testing. For the preparation of the modified porcelain composites (MPS) specimens, the neat porcelain was first mixed with different weight percentages 2 %, 4 %, and 6 wt% (MPS/FA2%, MPS/FA4%, and MPS/FA6%; respectively) of fly ash and specimens were prepared and treated at the same conditions as BPS. Fly ash (FA) used in this work was provided by Sika company. The main phases of fly ash XRF (X-ray fluorescence) technique is mullite phase (aluminum silicate compound, 28.4 %) and quartz (62.1 %), beside minor amount of other oxides (Fe_2O_3 , CaO , MgO , SO_3 , K_2O , P_2O_5 and TiO_2). Fig. 1 shows the image of different molded samples.

3. Morphological and structural characterization of porcelain composites

3.1. X-ray diffraction (XRD) analysis

The crystalline phases of the prepared porcelain specimens have been identified and confirmed in this work using XRD analysis, Bruker.

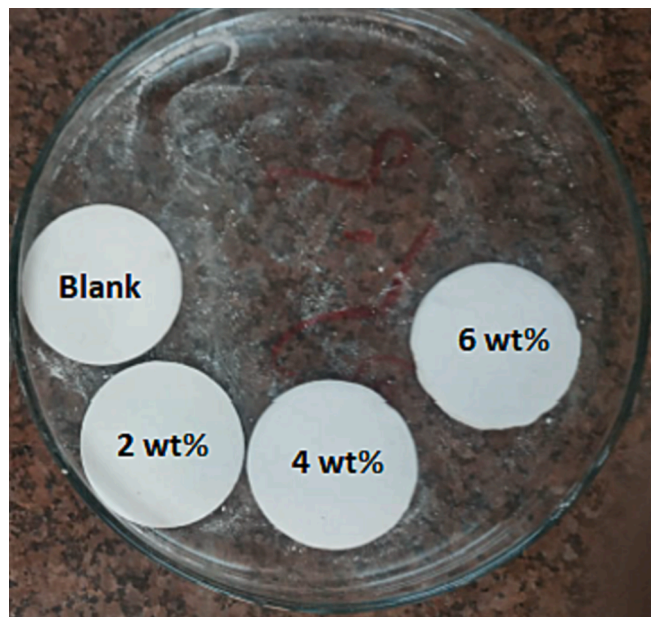


Fig. 1. Blank porcelain sample and modified porcelain composites.

D8 Advance Cu $\text{K}\alpha$ target with secondary nano chromator and installed by Cu Target X-ray tube and Geiger Muller tube. The settings used for tube run were at 30 kV, 15 mA divergence, receiving and scatter slides, 1,1 cm and 1; respectively and chart speed 100c.p.s. Fig. 2 presents the XRD pattern of blank porcelain sample (BPS) sintered at 1200 °C. The obtained intensity and diffraction angle of the peaks are matched with that as introduced in [11]. The obtained X-ray patterns indicated the existence of mullite ($3\text{Al}_2\text{O}_3 \cdot 2\text{SiO}_2$) at about $\sim 2\theta = 16.44^\circ$, 26.02° , 26.33° , 31.1° , 33.2° , 35.22° , 40.086° and 41.01° . Also, quartz (SiO_2) was detected by its diffractions at $\sim 2\theta = 20.84^\circ$, 26.62° , 39.41° , and 60° . The XRD diffraction patterns of modified porcelain samples with 4 % fly ash and with 6 % fly ash sintered at 1200 °C are presented in Fig. 3 and Fig. 4. Comparing with XRD analysis of fly ash that was reported previously [15], the obtained XRD peaks of the modified porcelain composites indicated the same diffraction patterns as neat porcelain and confirmed the attachment of the microparticles additives (fly ash) with the porcelain structure.

3.2. Scanning electron microscopy (SEM)

The morphological feature of porcelain sample and modified porcelain composites with 4 % and 6 % fly ash were examined after sintering at 1200 °C we investigated using SEM Model Quanta 250 Field Emission Gun connected with Energy Dispersive X-ray Analyzer, under 30 kV accelerating voltage, magnification 14x up to 10^6 and resolution for Gun. 1n. The SEM image of neat sample (25 % quartz + 50 % kaolin + 25 % feldspar) displayed the existence bushy matrix of amorphous quartz that discovered as petites with different shadows (gray and black) and millet dispersed along the hyaline matrix. Some pores have been detected along this matrix as a black small zones the images of SEM, Fig. 5. The microstructure of modified porcelain composites with 4 % and 6 % fly ash are presented in Figs. 6 and 7, respectively. The scanned images for these composites confirmed with the positive impact of fly ash on the densification of the formed matrix, as it demonstrated highly dense and compact microstructure compared to neat porcelain with nearly no pores present (Figs. 6 and 7). These results confirmed and agreed with the obtained data of porosity, bulk density, and water absorption.

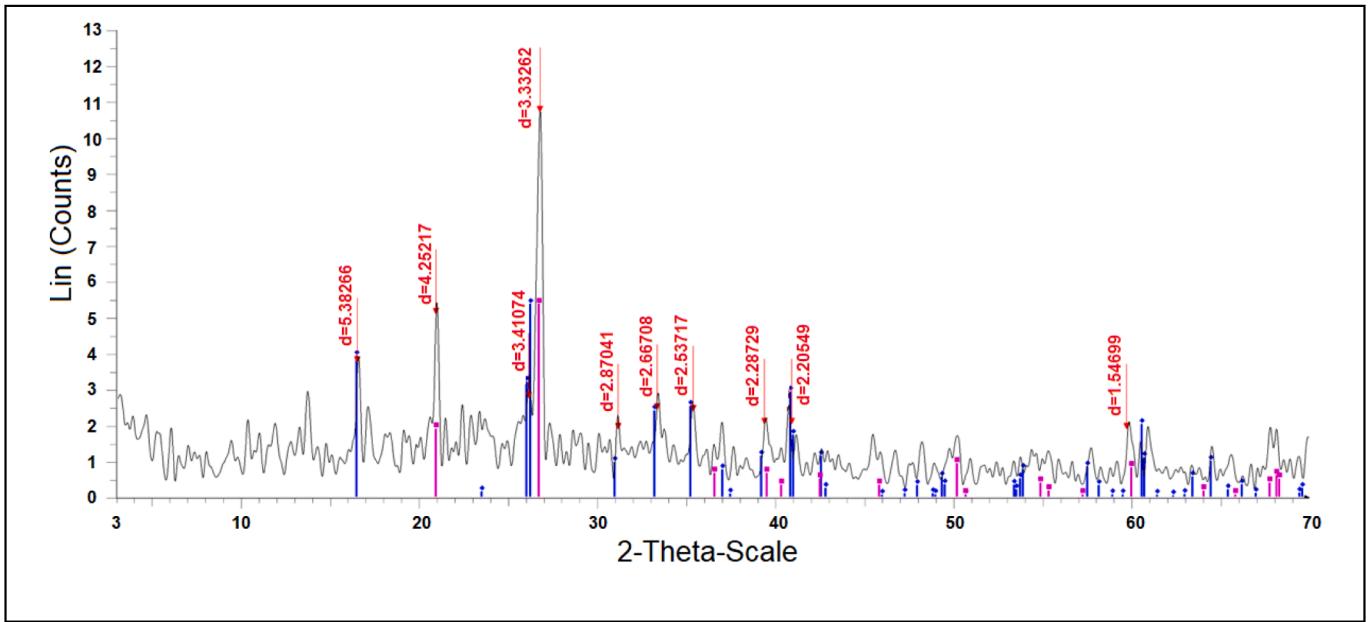


Fig. 2. XRD analysis for blank porcelain sample sintered at 1200 °C.

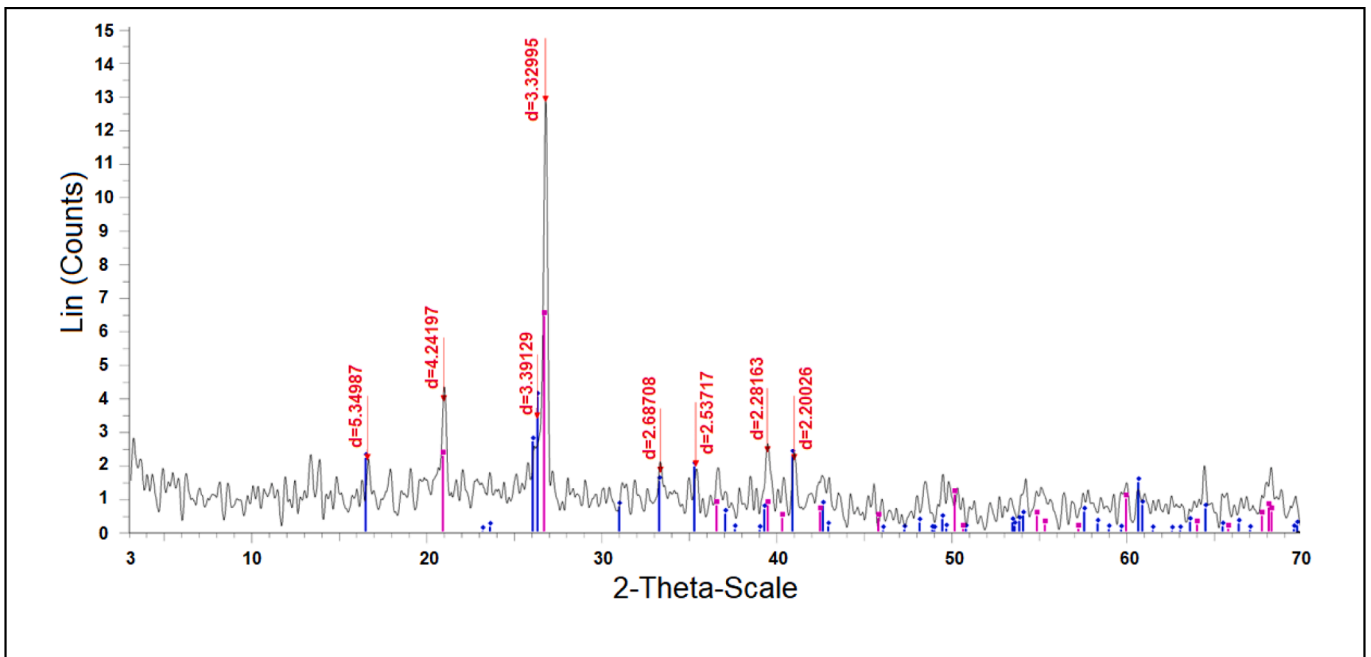


Fig. 3. XRD analysis for modified porcelain sample with 4% fly ash sintered at 1200 °C.

4. Dielectric properties of porcelain composites

4.1. Breakdown voltage

Highly withstand voltage of dielectric material provides reliable operation of electrical system due to the minimization of insulation failure probability. In contrast, low values of breakdown voltage (BDV) refer to a certain problem in the insulator that menace the continuity of supply [16]. Therefore, the highly important characteristic of the porcelain insulator is the breakdown voltage (withstand voltage). The AC breakdown voltage (AC BDV) in this work had been measured with the application of AC voltage using sphere-to-sphere copper electrodes. The porcelain specimen was fixed between these electrodes and immersed in

highly insulating liquid, as shown in Fig. 8, to eliminate the occurrence of flashover on the specimen surface. The range of voltage that applied is from 0 to 60 kV with 2 kV/s ramp rate.

Weibull distribution analysis is introduced to evaluate all probabilities for AC BDV to introduce dielectric failure analysis using few number of measurements. Weibull cumulative probability function can be illustrated as [16]:

$$F(v, \alpha, \beta) = 1 - e^{-\left(\frac{v}{\beta}\right)^\alpha} \quad (1)$$

where, breakdown voltage is v (kV), Scale parameter is β (kV), and Shape parameter is α . The shape parameter and scale parameter can be evaluated via linear retraction. Accordingly, the cumulative

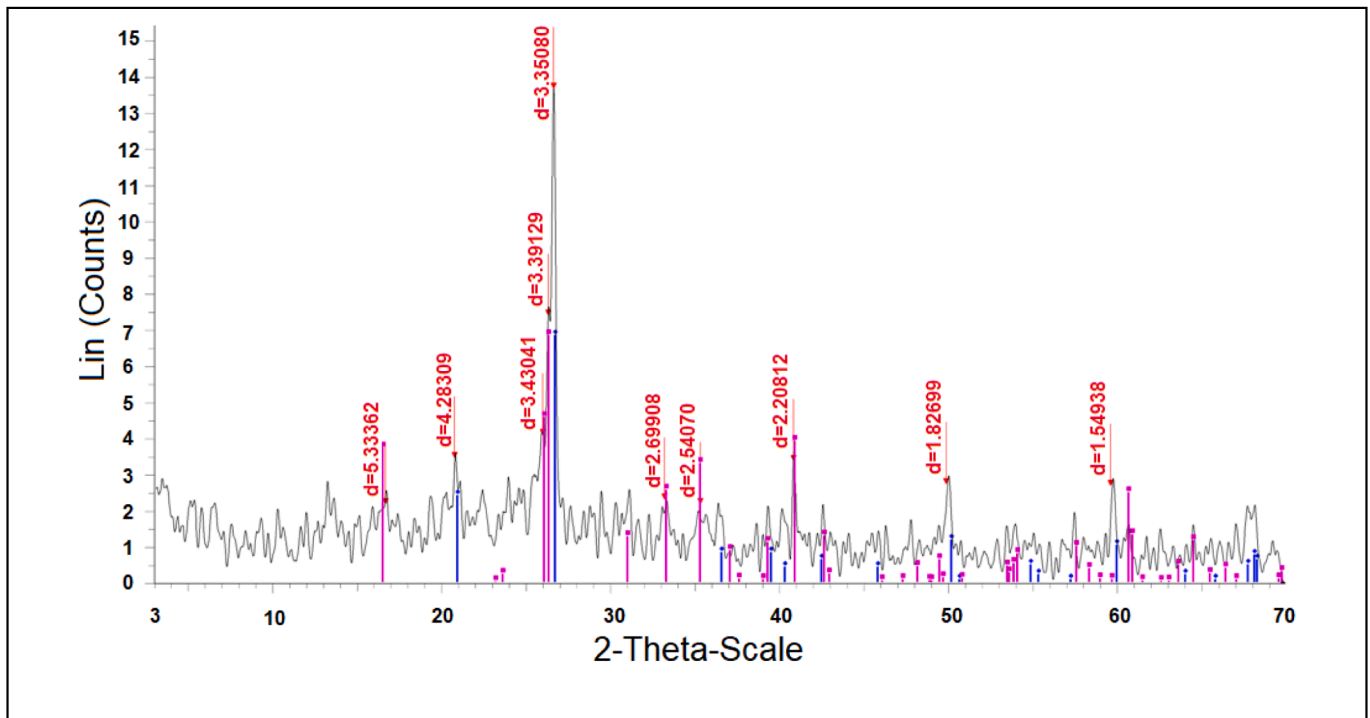


Fig. 4. XRD analysis for modified porcelain sample with 6% fly ash sintered at 1200 °C.

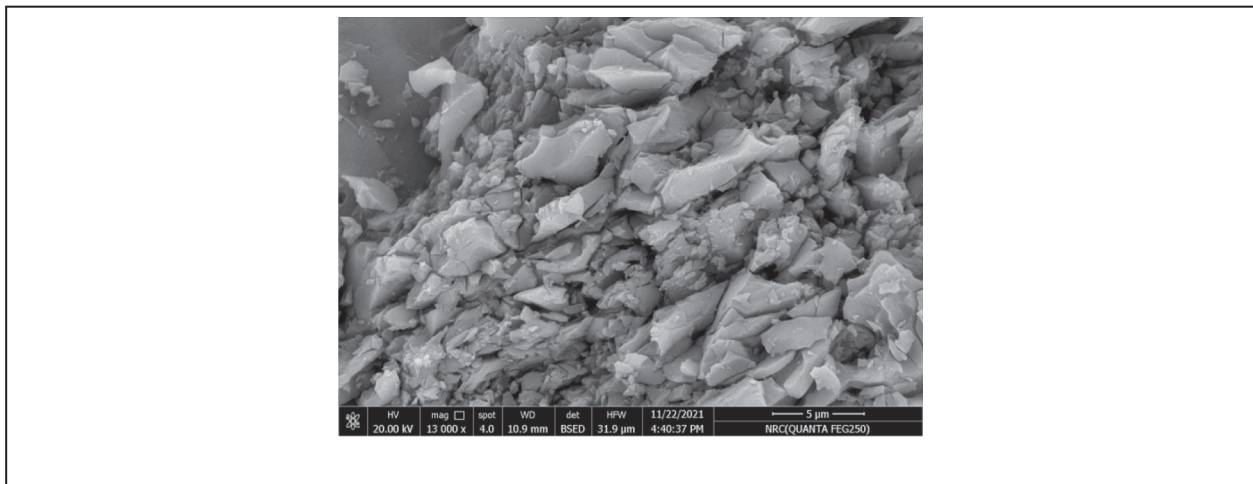


Fig. 5. SEM image for neat porcelain sample sintered at 1200 °C.

probabilities can be obtained. The cumulative probabilities of Weibull ranking for blank porcelain sample and modified porcelain composites are presented in Fig. 9. Further, Weibull parameters and the AC breakdown voltage for 50 % probability have been introduced as shown in Table 1. The AC BDV for 50 % probability is an indication for the average value of the obtained tested results.

At 50 % probability, the AC BDV of the blank porcelain sample is 22.5 kV. The addition of Fly Ash with weight percentage 2 %, 4 %, and 6 % cause an increasing of AC BDV from 22.5 kV to 29.5 kV, 51.1 kV, and 56.7 kV respectively. From the tested results, it is seen that, the higher loading of fly ash additives the higher AC BDV of the porcelain sample. These ameliorations can be imputed to the hurdle effect of the fly ash additives established in the matrix of porcelain material. Fly ash additives are considered as barrier points that resist the flow of electric charge carriers. The breakdown conducting path will be elongated and directed along the fly ash additives surface. So, the larger loading of fly

ash the larger surface of the breakdown path the higher breakdown voltage [17].

Now, there is a very important question. Is more increasing of the fly ash additives causes a more improvement for the dielectric properties of porcelain composite? To can discuss the answer for this important question, another two samples were prepared with fly ash percentage of 8 % and 10 %. These two porcelain samples were tested under breakdown test. the obtained average AC BDV recorded as 30 kV and 17 kV for the samples of 8 % and 10 %, respectively. According to these results, there is a constrains for the weight percentage of the fly ash additives. This constrain can be returned to make the fly ash additives be highly spread inside the blank porcelain matrix and not agglomerated as presented in the case of highly loading of fly ash additives (8 % and 10) that reversely impact on the dielectric characteristics. So, this paper limited to study the lightly concentrations of fly ash additives with wt% range from 2 % to 6 %.

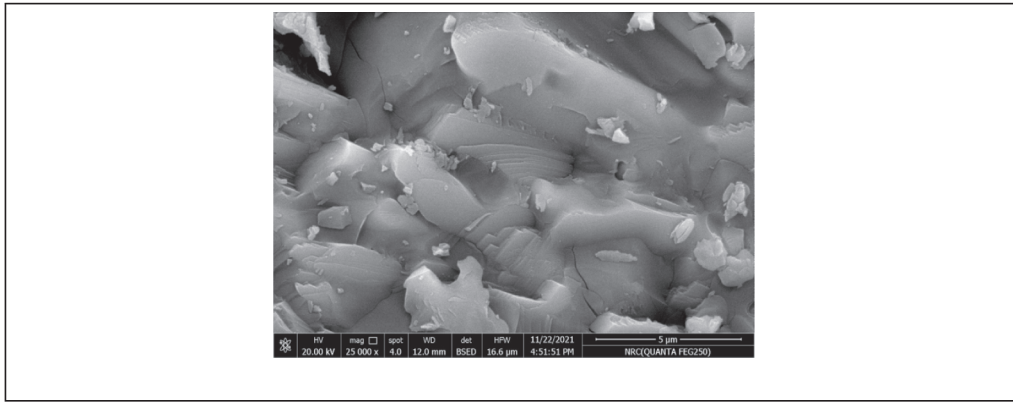


Fig. 6. SEM image for modified porcelain sample with 4% fly ash sintered at 1200 °C.

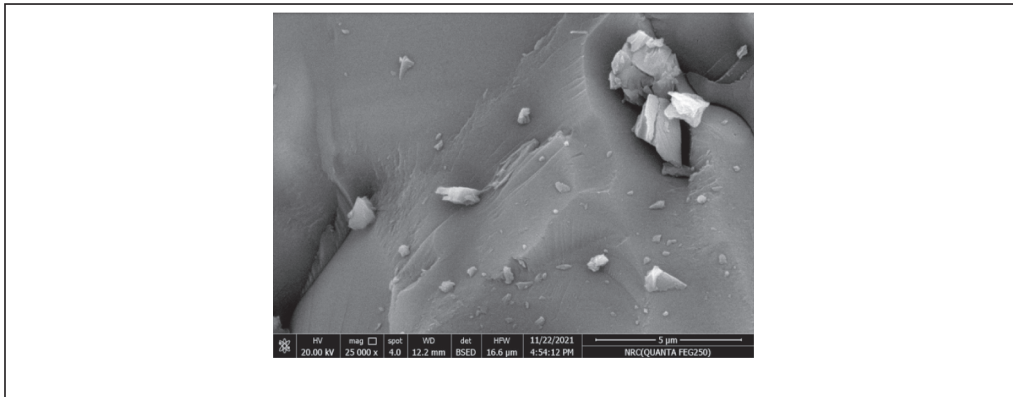


Fig. 7. SEM image for modified porcelain sample with 6% fly ash sintered at 1200 °C.



Fig. 8. AC breakdown tester with the tested porcelain specimen.

4.2. Permittivity and dissipation factor

The dissipation factor of any insulating material is an important factor, this factor refers to the dielectric losses into this insulation, thus, it be an index for the quantity of contaminations and impurities inside it [18]. On the other hand, the permittivity of the insulation (ϵ_r) refers to

its ability to store electrical energy in the presence of electric field due dielectric polarization. The value of dissipation factor (DF) can be evaluated as the ratio of the dielectric loss (ϵ'') to the dielectric coefficient (ϵ') [19]. These relations can be summarized as the following Eqs. ((2)–(5)).

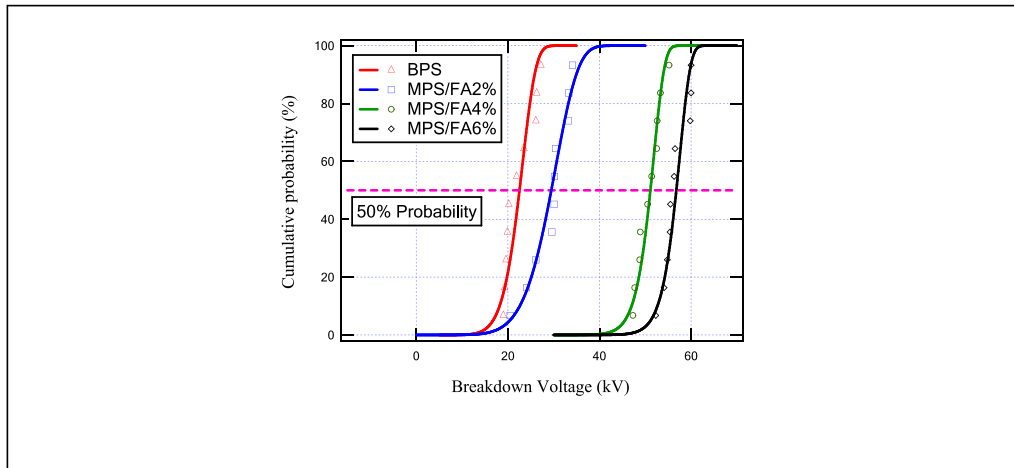


Fig. 9. Weibull distribution analysis for blank porcelain sample and modified porcelain composites.

Table 1

Weibull distribution analysis results for all samples at frequency of 50 Hz.

Porcelain sample	β	α	BDV _{50%}
BPS	23.50	8.78	22.5
MPS/FA2%	31.05	7.08	29.5
MPS/FA4%	51.95	22.52	51.1
MPS/FA6%	57.61	25	56.7

$$\epsilon_r = \epsilon' - j\epsilon'' \quad (2)$$

$$\tan\delta = \frac{\epsilon''}{\epsilon'} \quad (3)$$

$$\epsilon' = \frac{dC_p}{\epsilon_o A} \quad (4)$$

$$\epsilon'' = \frac{d}{2\pi f \epsilon_o A R_p} \quad (5)$$

LCR meter was used in this work to measure the capacitance (C_p) and resistance (R_p) of the porcelain specimen with thickness (d) and electrode CSA (A) via frequencies from 20 Hz to 1×10^6 Hz at normal room temperature. The obtained values of the dielectric parameters for the prepared samples at frequency 50 Hz are presented in Table 2. Moreover, the changing of the relative permittivity and the variation of dissipation factor due to these frequencies can be presented respectively, as shown in Figs. 10,11.

From the obtained results, regarding to the relative permittivity, the addition of fly ash with weight percentage 2 %, 4 %, and 6 % cause a decreasing in its value from 10.22 to 9.41, 7.17, and 7.243 respectively. while, the dissipation factor decreased from 0.113 to 0.028 via the fly ash loading. This can be attenuated to, the constructed bonds between fly ash and porcelain matrix have lower mobility that decrease the polarization between them [20]. Consequently, the addition of fly ash inside the porcelain base matrix improve its dielectric properties, not only the relative permittivity but also the dissipation factor.

Table 2

Dielectric parameters for all prepared samples at 50 Hz.

Sample ID	ϵ''	ϵ'	ϵ_r	DF
BPS	1.15	10.16	10.22	0.113
MPS/FA2%	0.65	9.39	9.41	0.069
MPS/FA4%	0.36	7.16	7.17	0.051
MPS/FA6%	0.203	7.24	7.243	0.028

5. Physical characteristics of porcelain compositions

Evidently, the most important physical property of any insulating solid material is its porosity and consequently its water absorption ability and bulk density. The higher the porosity of the insulator, the probability of insulation failure increases. The presence of many pores with various diameters along the insulating material promoted its absorption for moisture and contaminations that deteriorate its dielectric and thermal properties [20]. So, this work focused on decline the porosity of porcelain via admixing it with various amount of fly ash macro-particles. Porosity (P), Bulk Density (BD) (g/cm^3) and Water Absorption (WA) were evaluated based on Archimedes method following to ASTM C20 [21]. The following equations were used.

$$P = \frac{w_w - w_d}{w_w - w_s} \quad (6)$$

$$BD = \frac{w_d}{(w_w - w_s)} \quad (7)$$

$$WA = \frac{w_{sb} - w_d}{w_d} \quad (8)$$

where;

- w_w = wet weight of the sample.
- w_d = dry weight of the sample.
- w_s = suspended immersed in water weight of the sample.
- w_{sb} = soaked weight after boiling at 100 °C for 2 h.

Fig. 12, presents the porosity of the prepared porcelain samples at different sintering temperatures. At 1200 °C, the porosity of blank porcelain sample is 0.712 %. The presence of different doses of fly ash inside the porcelain matrix notably decreases its porosity. The porosity of the samples MPS/FA2%, MPS/FA4%, and MPS/FA6% are 0.38 %, 0.287 %, and 0.103 % respectively. The observed decline in porcelain porosity is returns to the filling effect of fly ash macro-particles for the present pores, producing more closely mobilized porcelain matrix with lower water absorption and higher density values compared with the blank one [22,23]. The values of water absorption (WA) and bulk density (BD) for the prepared samples are presented at different temperatures in Fig. 13 and Fig. 14 respectively. Moreover, these measured physical parameters are summarized in Table 3 at 1200 °C (selected as optimum sintering temperature). The results indicated that the lower porosity is accompanied by the higher density and lower water absorption values.

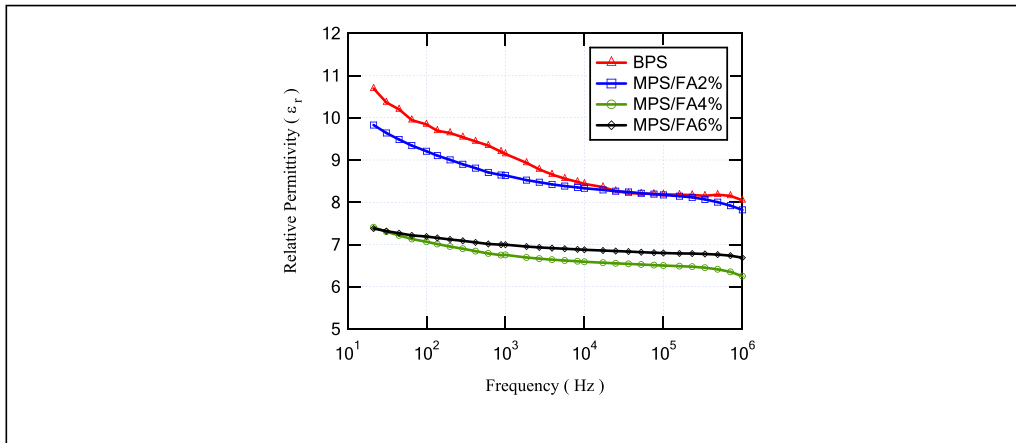


Fig. 10. Relative permittivity versus frequency for all porcelain samples.

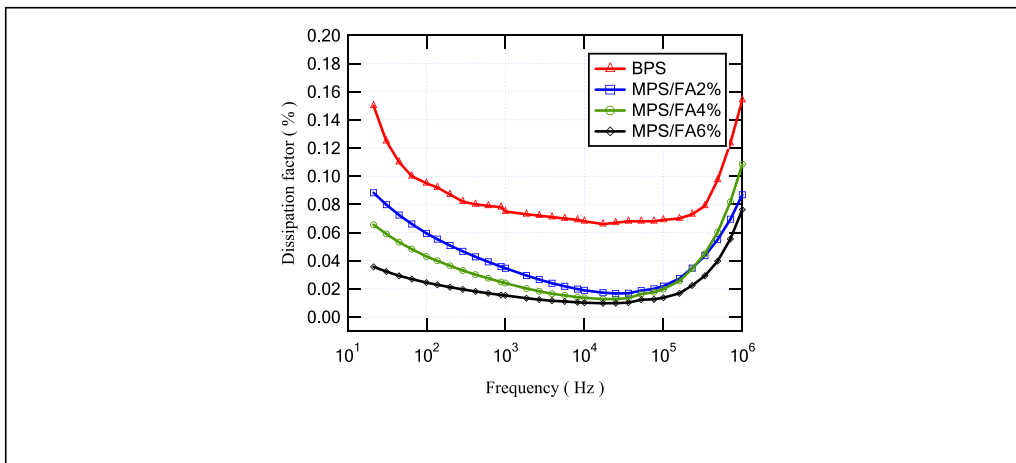


Fig. 11. Dissipation factor versus frequency for all porcelain samples.

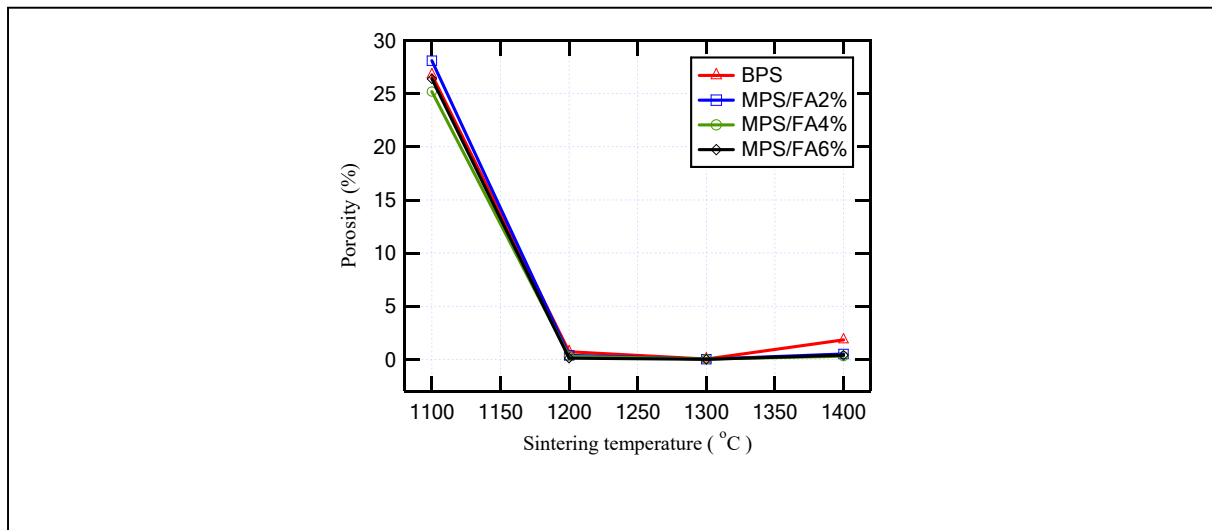


Fig. 12. Porosity for all porcelain samples at different sintering temperature.

6. FEM analysis using comsol multiphysics software

As known, FEM (Finite Element Method) is a widely recognized numerical method that empowers to tackle complex numerical

problems. FEM is more recommended than other numerical methods according to its many advantages [24]. These advantages can be summarized as: (i) easier modeling of complex geometrical and irregular shapes, (ii) high degree of accuracy, (iii) saving time for a large number

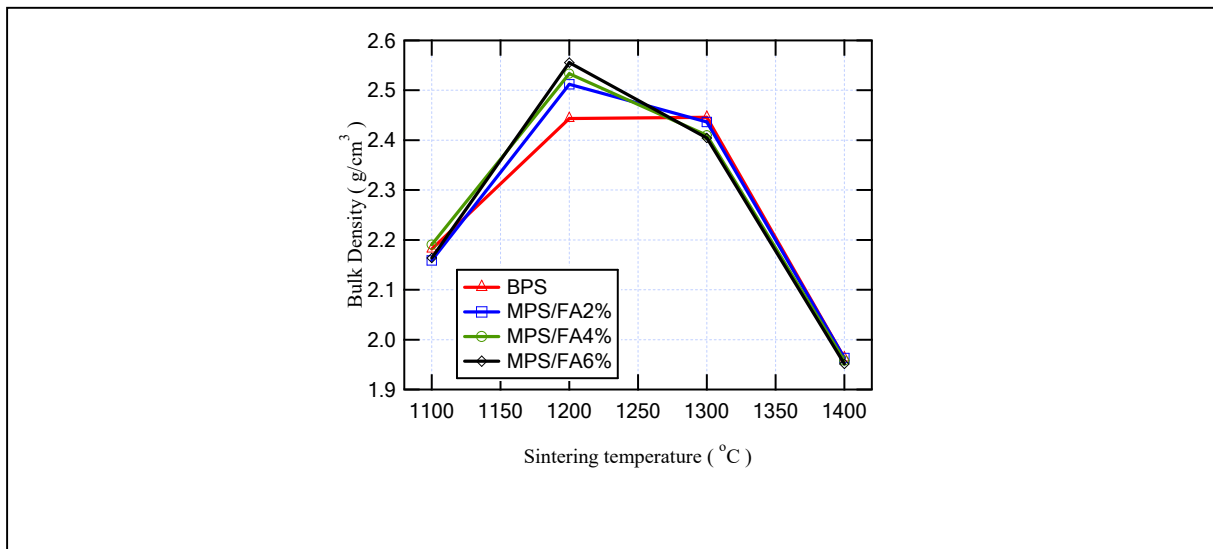


Fig. 13. Bulk density for all porcelain samples at different sintering temperature.

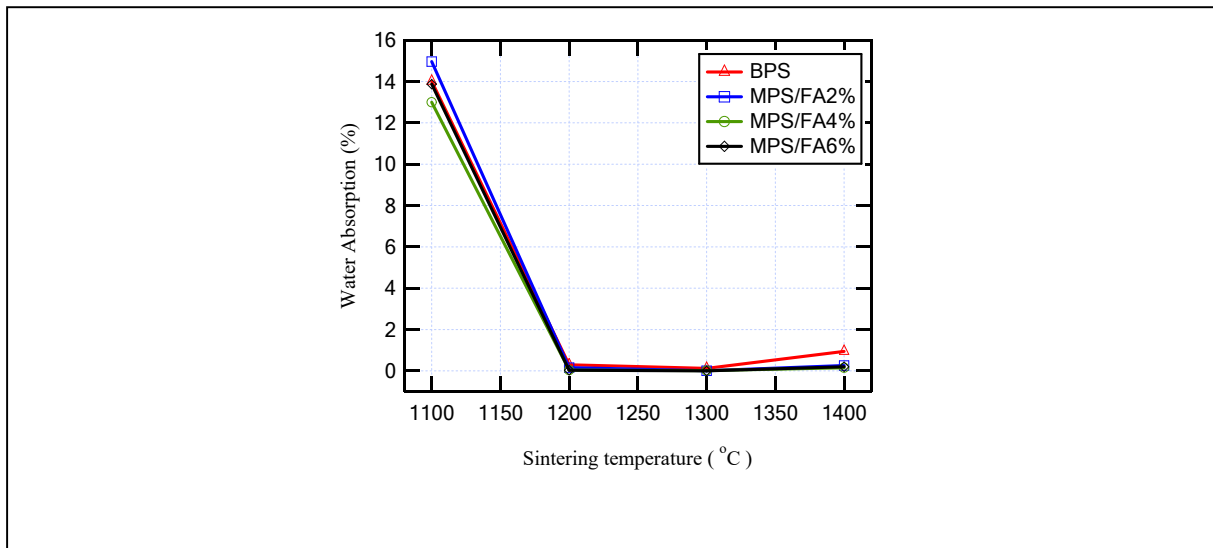


Fig. 14. Water absorption for all porcelain samples at different sintering temperature.

Table 3
Measured physical parameters for all samples at 1200 °C.

Sample ID	Porosity (%)	Bulk density (g/cm ³)	Water absorption (%)
BPS	0.712	2.4432	0.2926
MPS/FA2%	0.380	2.5123	0.1567
MPS/FA4%	0.287	2.5331	0.0369
MPS/FA6%	0.103	2.5557	0.0438

of iterations, (iv) easy detection of any defect in the model from the detailed visualizations [24,25]. In this section, a 2D stationary study using COMSOL Multiphysics Software is introduced. This study simulates the distribution of electric fields on porcelain samples using FEM. Average breakdown voltage, relative permittivity, dissipation factor, porosity, water absorption, and blank density are entered as input parameters for the simulated model. The applied Multiphysics mode is the electrostatic mode based on the finite element method. The considered model is a sphere-to-sphere separated with the porcelain sample and immersed in an insulating oil to avoid flashover as presented in Fig. 15.

COMSOL Multiphysics Software-based FEM compiled to depend on the field region that is divided into fine smaller triangle zones to dwindle the energy over the spacious field region with the applying of the numerical FEM [26,27]. Under the application of stationary electric field, the following equations (9)–(13) deliver the electrical energy W stored inside the full volume U of the area under study, taking into consideration the spherical model geometry as well as the Laplacian field. According to variational calculus, the FEM is mainly dependent on the fact that Laplace or Poisson equations are assured when the total energy functional is minimal [28].

$$w = \frac{1}{2} \int_U \epsilon |\text{grad}(V)|^2 \cdot dU = \frac{1}{2} \int_U \epsilon (\nabla \cdot \nabla V) \cdot dU \quad (9)$$

$$w = \frac{1}{2} \iiint_U \left[\epsilon_r \left[\frac{1}{r^2} \times \frac{\partial}{\partial r} \left(r^2 \frac{\partial V}{\partial r} \right) \right] + \epsilon_\theta \left[\frac{1}{r^2 \sin \theta} \times \frac{\partial}{\partial \theta} \left(\sin \theta \frac{\partial V}{\partial \theta} \right) \right] + \epsilon_\varphi \left[\frac{1}{r^2 \sin^2 \theta} \times \frac{\partial^2 V}{\partial \varphi^2} \right] \right] \times (r^2 \sin \theta \times dr d\theta d\varphi) \quad (10)$$

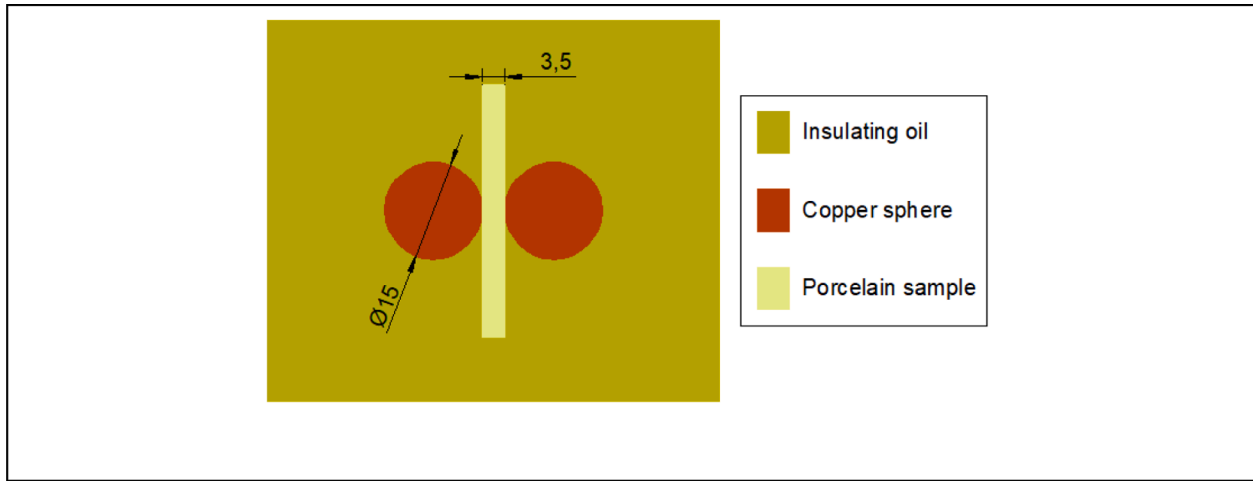


Fig. 15. The simulated model with millimeters dimensions.

$$\frac{w}{\theta} = \frac{1}{2} \times \epsilon \iint_A \left[\left[\frac{\sin\theta}{r} \times \frac{\partial}{\partial r} \left(r^2 \frac{\partial V}{\partial r} \right) \right] + \left[\frac{1}{r \sin\theta} \times \frac{\partial^2 V}{\partial \varphi^2} \right] \right] \times dr d\varphi \quad (11)$$

$$\frac{w}{\theta} = \frac{1}{2} \times \epsilon \sum_{i=1}^n \left[\left[\frac{\sin\theta}{r} \times \frac{\partial}{\partial r} \left(r^2 \frac{\partial V}{\partial r} \right) \right] + \left[\frac{1}{r \sin\theta} \times \frac{\partial^2 V}{\partial \varphi^2} \right] \right] \cdot dA_i \quad (12)$$

$$\vec{E} = -\nabla V = -\vec{i} \frac{\partial V(r, \varphi)}{\partial r} - \vec{k} \frac{\partial V(r, \varphi)}{\partial \varphi} \quad (13)$$

in which $(\nabla^2 \cdot \mathbf{V} = 0)$, $((w) / (\theta))$, ϵ , n , and A_i denote the Laplacian equation, followed by the energy density per unit length for elementary area dA , in addition, the permittivity of the sample material, then the total number of elements, followed by the area of the i^{th} triangle element, respectively. For more flexibility, the energy reduction formulation within the whole system might be entered as $(\partial w / \partial V = 0)$ [28]. Moreover, this approximation should be utilized at the unknown potential nodes to compute the electrostatic potential, after that the electric field strength E can be easily calculated by equation (13) [29]. Accordingly, Fig. 16(a) shows the model after the creation on the COMSOL Multiphysics software window with the selection of 2D space dimension [30]. Moreover, Fig. 16(b) presents the mesh construction of FEM size to analyze the model.

The simulation has been compiled for the blank porcelain sample (BPS). Fig. 17 presents the electric field distribution due to the applied breakdown voltage that measured for BPS (22.5 kV). From the obtained results, the hot spot can be cleared at the point that touched between the spherical HV electrode and the porcelain sample. The electric field at this point is 46.5 kV/mm.

The simulation has been repeated for all porcelain samples (BPS, MPS/FA2%, MPS/FA4%, and MPS/FA6%). From the simulation obtained results, the maximum value of electric field that appeared on each porcelain sample can be presented in Fig. 18. The electric field closely the tip of the spherical electrode is increased with the increasing of the fly ash concentration. These values present the enhancement of the breakdown strength of the porcelain insulating material. The enhancement of the dielectric properties of the porcelain insulating material achieved an improvement compared to BPS with 18.5 %, 48 %, and 66 % compared for 2 %, 4 %, and 4 % fly ash concentration, respectively.

7. Conclusions

This study focused on evaluating the effect of admixing porcelain material with fly ash microparticles on its dielectric and physical properties.

The following outcomes can be derived:

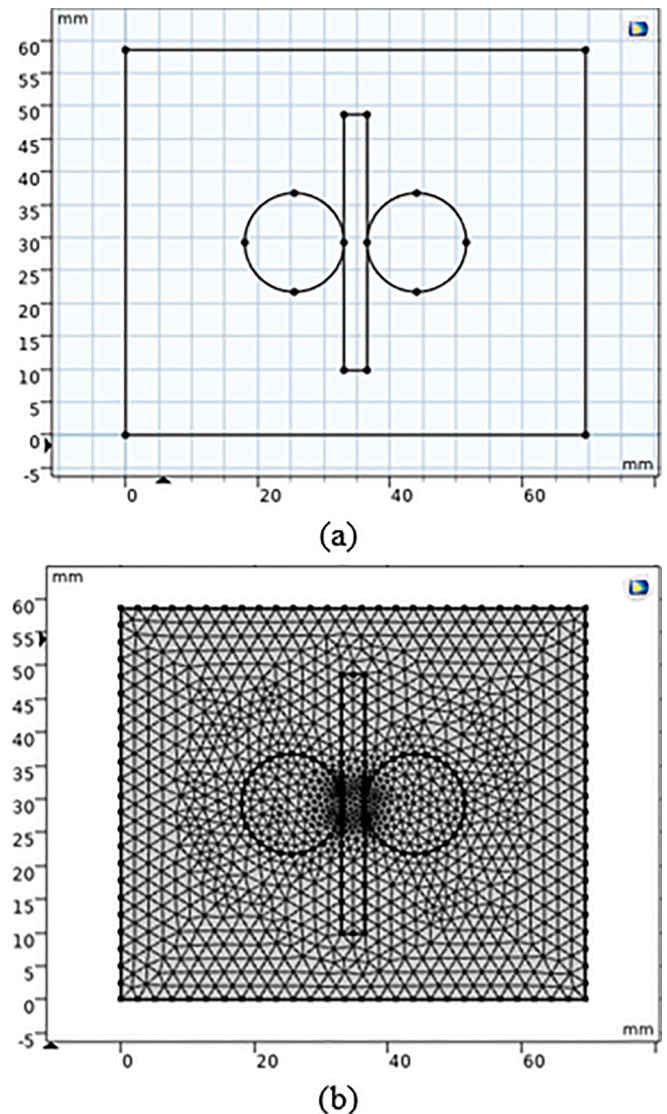


Fig. 16. The simulated model with 2D space dimension on COMSOL software. (a) without mesh presentation, (b) with mesh presentation.

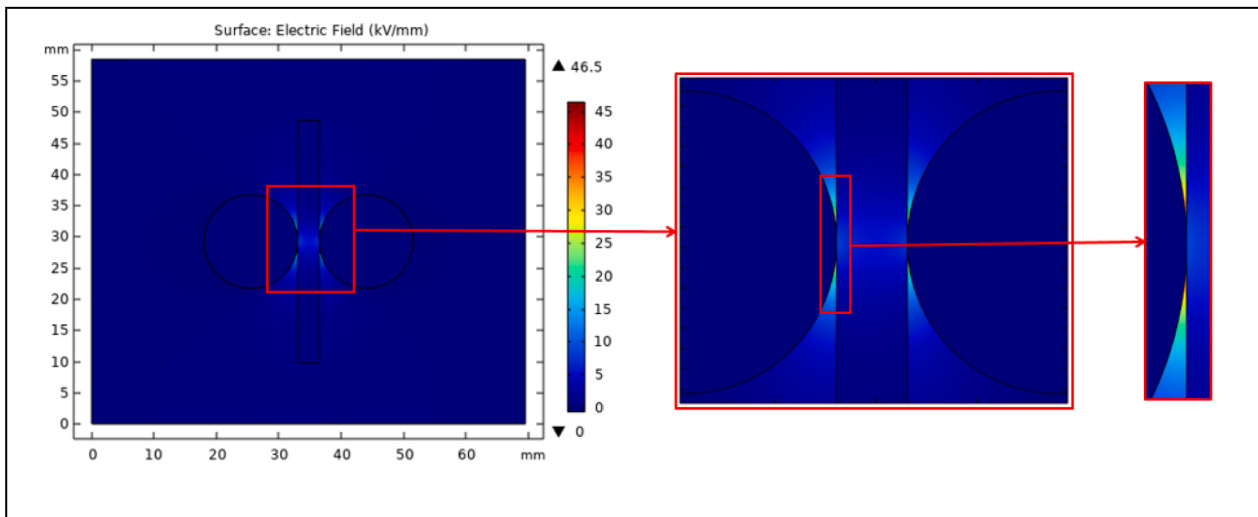


Fig. 17. Electric field distribution on the blank porcelain sample.

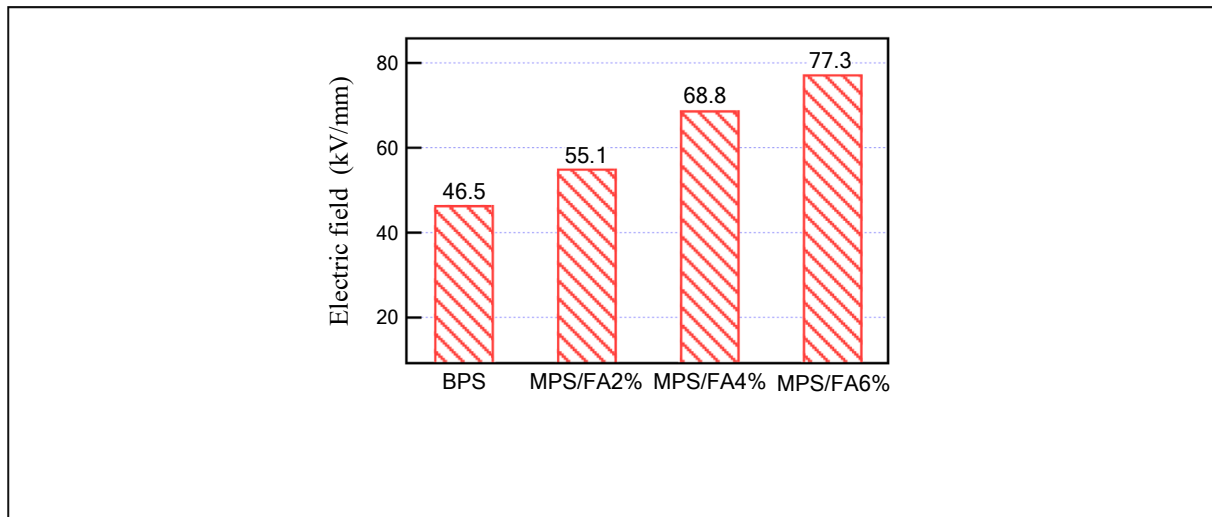


Fig. 18. Maximum electric field appeared on each porcelain sample.

1. Regarding the breakdown voltage, with the weight percentage loading of fly ash from 2 % to 6 %, the breakdown voltage increased from 29.5 kV to 56.7 kV. The increasing of breakdown voltage is assigned to the barrier effect of the fly ash additives embedded in the porcelain matrix.
2. Regarding the relative permittivity and dissipation factor, the presence of the fly ash inside the porcelain matrix causes a decreasing of relative permittivity and dissipation factor. This decrement is due to the lower mobility of the carrier charges for the modified porcelain compositions.
3. Regarding the porosity of the prepared porcelain samples, the adding of fly ash with 2 %, 4 %, and 6 % reduce the porosity with 45 %, 54 %, and 98 % compared to the blank porcelain sample. This returns to the formation of a more closely packed porcelain matrix which was assigned to the pore filling effect of fly ash micro-particles.
4. Simulation using COMSOL Multiphysics was introduced to clarify the distribution of electric field inside each porcelain sample. The simulated results revealed that the breakdown strength of porcelain samples was increased (from 46.5 to 77.3 kV/mm) with the increasing of the fly ash loading inside porcelain matrix.

References

- [1] L.U. Anih, "Indigenous manufacturer and characterization of electrical porcelain insulator," *Nigerian Journal of Technology*, vol. 24, no. 1, 2005.
- [2] S. Jin, W. Mo, J. Wei, and et al., "Analysis and verification of strength of 110kV porcelain post insulator," *IEEE 4th Inter. Conf. Electric Power Equipment - Switching Technology (ICEPE-ST)*, China, 2017.
- [3] Belhouchet K, Bayadi A, Belhouchet H, Remero M. Improvement of mechanical and dielectric properties of porcelain insulators using economic raw materials. *Boletín De La Sociedad Española De Cerámica y Vidrio* 2019;58(1):28–37.
- [4] Olupot P, Jonsson S, Byaruhanga J. Study of glazes and their effects on properties of triaxial electrical porcelains from Ugandan minerals. *J Mater Eng Perform* 2010; 19:1133–42.
- [5] Aigbodion V, Achiv F, Agunsoye O, Isah L. Evaluation of the electrical porcelain properties of alumina-silicate nano-clay. *J of the Chinese Advanced Materials Society* 2015;4:99–109.
- [6] E. Contreras, M. Gallaga, and E. A. Rodriguez, "Effect of nanoparticles on mechanical and electrical performance of porcelain insulator," *IEEE Conf. on Elect. Insul. and Dielec. Phenom. (CEIDP)*, Canada, 2016.
- [7] Goeuriot D, Belnou F, Goeuriot P, Valdivieso F. Nanosized alumina from boehmite additions in alumina porcelain. Part 1: Effect on reactivity and mullitisation. *Ceramics Int* 2004;30:883–92.
- [8] Goeuriot D, Belnou F, Goeuriot P, Valdivieso F. Nanosized alumina from boehmite additions in alumina porcelain. Part 2: Effect on material properties. *Ceramics Int* 2007;33:1243–9.
- [9] Zhuang J, Liu P, Dai W, Fu X. A novel application of nano anticontamination technology for outdoor high-voltage ceramic insulators. *Int J Appl Ceram Technol* 2010:46–53.

- [10] Yuruyen S, Toplan H. The sintering kinetics of porcelain bodies made from waste glass and fly ash. *J Ceram Int* 2009;35:2427–33.
- [11] Desouky OA, Belal E, El-Gamal SMA, Abd-Allah MA, Eliyan T. Improving the insulating and physical characteristics of HV porcelain dielectric materials using nano-silica. *J Mater Sci: Mater Electron* 2020;31:12649–60.
- [12] Zhuang J, Liu P, Dai W, Fu X, Li H, Zeng W, et al. A novel application of nano anticontamination technology for outdoor high-voltage ceramic insulators. *Int J Appl Ceram Technol* 2010;7:E46–53.
- [13] Z. Wu, J. Li, Y. Wei, Z. Huang, X. Yan, and J. Zhang, "Influence of nano boron nitride (BN) on electric corrosion of fluororesin based super hydrophobic coatings for insulators," IEEE Inter. Conf. on High Voltage Eng. and Appl. (ICHVE), China, 2016.
- [14] Alterary SS, Marei NH. Fly ash properties, characterization, and applications: a review. *Journal of King Saudi University-Science* 2021;33(6):101536.
- [15] M.L. Mings, S.M. Schlorholtz, J.M. Pitt, and T. Demirel, "Characterization of Fly Ash by X-Ray Analysis Methods", Transportation Research Record 941, pp. 5-11.
- [16] D. A. Mansour, E. A. Shaalan, S. A. Ward, A. Z. El-Dein, and H. S. Karaman, "Multiple Nanoparticles for Enhancing Breakdown Strength and Heat Transfer Coefficient of Oil Nanofluids," IEEE Inter. Middle East Power Systems Conf. (MEPCON), pp. 1406-1410, Egypt, 2017.
- [17] W. Yan, B. T. Phung, Z. J. Han, and K. Ostrikov, "Surface Insulation Performance of Epoxy Resin/Silica Nanocomposite Material," IEEE Electrical Insulation Conference, Annapolis, Maryland, 2011.
- [18] Mansour DA, Shaalan EA, Ward SA, El-Dein AZ, Karaman HS, Ahmed HM. Multiple nanoparticles for improvement of thermal and dielectric properties of oil nanofluids. *IET Sci Meas Technol* 2019;13(7):968–74.
- [19] Karaman HS, Ahmed HM, Darwish MMF, Mansour DA. The effect of geraphene on the thermal and dielectric properties of epoxy resin. *IEEE Inter Symp Electr Insul Mater (ISEIM)*, Japan 2020.
- [20] Abdel-Gawad NMK, El-Dein AZ, et al. Enhancement of dielectric and mechanical properties of polyvinyl chloride nanocomposites using functionalized TiO2 nanoparticles. *IEEE Trans Dielectr Electr Insul* 2017;24(6):3490–9.
- [21] Astm. C20, standard test methods for apparent porosity, water absorption, apparent specific gravity and bulk modulus of burned refractory brick and shapes. *ASTM International* 2010.
- [22] Liu J, Gan D, Hu C, Kieme M, Ho PS, Volksen W, et al. Porosity effect on the dielectric constant and thermomechanical properties of organosilicate films. *Appl Phys Lett* 2002;81(22):4180–2.
- [23] Mehta NS, et al. Effect of sintering on physical, mechanical, and electrical properties of alumina-based porcelain insulator using economic raw materials doped with zirconia. *J Aust Ceram Soc* 2019;55(4):987–97.
- [24] Arslan S, Bicen Y, Binarbasi Ö. Numerical analysis and application of electric field grading device for metal-enclosed switchgear. *SN Applied Sciences* 2021;3:1–11.
- [25] Logg A. Automating the finite element method. *Arch Comput Methods Eng* 2007; 14:93–138.
- [26] Abdel-Gawad NMK, El Dein AZ, et al. Development of industrial scale PVC nanocomposites with comprehensive enhancement in dielectric properties. *IET Sci Meas Technol* 2019;13(1):90–6.
- [27] Karaman HS, Mansour DA, Lehtonen M, Darwish MMF. Condition assessment of natural ester–mineral oil mixture due to transformer retrofilling via sensing dielectric properties. *Sensors* 2023;23(14):1–20.
- [28] Matthew N. O. Sadiku, "Elements of Electromagnetics", Oxford University Press Inc., UK, seventh edition, Book, Ch. 3, p. 83, 2018.
- [29] Ahmed HM, Abdel-Gawad NMK, Afifi WA, Mansour DA, Lehtonen M, Darwish MMF. A novel polyester varnish nanocomposites for electrical machines with improved thermal and dielectric properties using functionalized TiO2 nanoparticles. *Materials* 2023;16(19):6478.
- [30] COMSOL Multiphysics Reference Manual, © 1998–2019 COMSOL, Version: COMSOL 5.5, Available online: https://doc.comsol.com/5.5/doc/com.comsol.help.comsol/COMSOL_ReferenceManual.pdf (accessed on July 2021).



Sherif M.M. Sherif was born in Egypt, in 1986. He received the B.Sc. degrees in electrical engineering from the Faculty of Engineering at Shoubra, Benha University, Cairo, Egypt, in 2008 and crisis diploma from Faculty of Commerce at Ain Shams University Cairo, Egypt in 2019. Since 2009, He has been with Marine Units and Maintenance section in Petrogulfmiser company at Maadi, Cairo, Egypt. His research interests include high voltage engineering and improvement Characteristics of high voltage insulation.



S.M.A. El-Gamal was born in Cairo, Egypt, on Sept, 1966. She received her B.Sc., M.Sc. and Ph.D. degrees from Ain Shams University. Since 2018, she is a professor of physical chemistry and building materials at Chemistry Department, Faculty of Science at Ain Shams University. Her main research areas include construction and building materials, green cement and concrete, geopolymers, ceramic materials, nanomaterials and nanocomposites and their applications, blended cement and material science.



Naser Abdel-Rahim, Ph.D., currently holds the position of Professor in the Department of Electrical Engineering of Future University in Egypt. From 2013 to 2017 he had been a Professor with the Faculty of Engineering at Shoubra, Benha University, Egypt. He received both the M. Eng. and Ph.D. degrees from the Memorial University of Newfoundland in Canada, in 1989 and 1995, respectively. As an Assistant Professor at the United Arab Emirates University (UAEU) from 2000 till 2005, he obtained several research projects funding from the UAEU as well as from Asea Brown Boveri (ABB). Abdel-Rahim has numerous publications in international journals and refereed conferences, where he also served as a reviewer.



M.A. Abd-Allah was born in Cairo, Egypt, on august 16, 1961. He received his B.Sc., and M.Sc. degrees from Zagazig University, Egypt and Ph.D. degree from Cairo University, Egypt. Since 2003, he is a Professor of high Voltage Engineering at Faculty of Engineering at Shoubra, Benha University. His main research areas include Renewable energy resources protection and mitigation from high transient voltages, Electromagnetic fields assessment, measurement and mitigation, Transients on power system and mitigation tools, Protection systems of HVAC and HVDC networks with a high penetration of renewable resources.



Hesham S. Karaman was born in Egypt, in 1990. He received the B.Sc. and M.Sc. degrees in electrical engineering from the Faculty of Engineering at Shoubra, Benha University, Cairo, Egypt, in 2011 and 2015, respectively, and the Ph.D. degree in electrical engineering from the same faculty in 2019. Since 2011, he has been with the Electrical Engineering Department, Faculty of Engineering at Shoubra, Benha University, Cairo, Egypt. His research interests include high voltage engineering, power system restoration, Artificial Neural Networks, internal discharge analysis, polymer nanocomposites, nanofluids, and high voltage insulation technology.